JOURNAL OF Applied Polymer SCIENCE

Fabrication of Vertically Aligned Ferroelectric Polyvinylidene Fluoride Mesoscale Rod Arrays

Dongjin Kim,[1,2] Seungbum Hong,[1,2,3] Jongin Hong,[4] Yoon-Young Choi,[1,3] Jiyoon Kim,[1] Moonkyu Park,[1] Tae-hyun Sung,[5] Kwangsoo No[1]

[1]Department of Materials Science and Engineering, KAIST, Daejeon 305-701, Korea
[2]Material Science Division, Argonne National Laboratory, Lemont, Illinois 60439
[3]Nanoscience and Technology Division, Argonne National Laboratory, Lemont, Illinois 60439
[4]Department of Chemistry, Chung-Ang University, Seoul 156-756, Korea
[5]Department of Electrical Engineering, Hanyang University, Seoul 133-791, Korea
Correspondence to: S. Hong (E-mail: hong@anl.gov) or K. No (E-mail: ksno@kaist.ac.kr).

ABSTRACT: We have fabricated vertically aligned ferroelectric PVDF mesoscale rod arrays comprising β and γ phases using a 200 nm diameter anodized aluminum oxide (AAO) as the porous template. We could synthesize the ferroelectric phase in mesoscale rod forms by combining the well-established recipe for crystallizing the β phase using dimethyl sulfoxide (DMSO) at low temperature and template-guided infiltration processing for the rods using AAO. We measured the dimensions of the PVDF rods by scanning electron microscopy and identified the polymorph phases by X-ray diffraction and Fourier transform infrared spectroscopy. The length of the rods varied from 3.82 μm to 1.09 μm and the diameter from 232 nm to 287 nm when the volume ratio between DMSO and acetone changed from 5 : 5 to 10 : 0. We obtained well-defined piezoresponse hysteresis loops for all rods with remnant piezoresponse ranging from 2.12 pm/V to 5.04 pm/V and coercive voltage ranging from 2.29 V to 2.71 V using piezoresponse force microscopy. Our results serve as a processing platform for flexible electronic devices that need high capacitance and piezoelectric functionalities such as flexible memory devices or body energy harvesting devices for intelligent systems. © 2013 Wiley Periodicals, Inc. J. Appl. Polym. Sci. 130: 3842–3848, 2013

KEYWORDS: polyvinylidene (PVDF); piezoelectrics; mesoscale rods arrays; anodized alumina oxide (AAO)

Received 15 January 2013; accepted 12 April 2013; Published online 14 May 2013
DOI: 10.1002/app.39415

INTRODUCTION

Ferroelectric polymers have been widely studied for use in many applications, including electronic devices,[1–4] energy harvesters,[5] acoustic transducers,[6,7] sensors,[8,9] and actuators.[5–7] Their versatile properties, such as high flexibility, low processing temperatures, simple fabrication processes, and non-toxicity have made these materials viable as alternatives to classical ferroelectric ceramics. In particular, when ferroelectric materials are prepared as quasi-one-dimensional (1-D) nanostructure arrays or mesoscale structures with high aspect ratio, some exceptional properties are manifested; these properties have attracted increasing levels of attention in the fields of non-volatile memory devices and nano-generators.[10,11] The enlarged surface area per unit volume in such structures, with high aspect ratio, leads to remarkable chemical and thermal reactivity; the preferred orientation formed during crystallization contributes to the anisotropic properties.[12,13] Several fabrication methods, such as template wetting,[14,15] imprinting,[8,16] and block copolymer methods[17] have been introduced to realize these polymer arrays with high aspect ratio. Among those methods, the template wetting technique is the most common; it entails the synthesis of the desired material within the pores of a membrane, leading to the fabrication of nanostructures, or mesoscale structures with high aspect ratio. The use of porous anodic aluminum oxide (AAO) as a template is one of the most successful and industrially promising fabrication methods.[18] Since AAO has a long-range ordered architecture and a cost that is relatively lower than that of other templates, it has been widely used as a template material. Some studies have already introduced the fabrication of 1-D nanostructures or mesoscale structures of ferroelectric polymers.[19,20]

Among the ferroelectric polymer materials, polyvinylidene fluoride (PVDF) has been applied in many fields due to its excellent

Additional Supporting Information may be found in the online version of this article.

solution processing capability, flexibility, good ferroelectric, and mechanical properties, high chemical resistance, and good thermal stability.[21–23] The polymorphism of PVDF, by which we mean the transformation of one crystal form to another under certain conditions, is of significant importance for ferroelectric properties. PVDF has three major crystalline phases: non-polar α, polar β, and γ.[24] The crystalline phases are distinguished by the conformation of the chain backbone, which is composed of C–C bonds. The β phase has an all *trans* planar zigzag conformation (TTTT); the α phase has an alternating *trans* and *gauche* conformation (TGT G); and the γ phase has a conformation intermediate between those of the α and the β phases, consisting of a chain of three *trans* and one *gauche* conformation (*TTTGTTT* G). The α phase of PVDF is the most common phase because it is the thermodynamically most stable state,[25] but it is non-polar because the dipole moments of the two molecular chains in the unit cell are antiparallel. In contrast, the polar β phase is of the most interest for ferroelectricity because its crystal structure has a polar unit cell with a large dipole moment. The γ phase is also polar but its dipole moment is smaller than that of the β phase.

To date, several approaches have been introduced to obtain large amounts of the β phase within PVDF films.[26–28] In casting PVDF solution onto a substrate, the formation of the β phase is very sensitive to drying temperature,[29] rate of evaporation of the solvent,[30] and dipole moment of the solvent.[31,32] However, there have been only a few studies in which ferroelectric PVDF nanostructures or mesoscale structures with high aspect ratio were fabricated by casting the PVDF solution onto a template. Herein, we demonstrate vertically aligned ferroelectric PVDF mesoscale rods and investigate their crystalline phases, piezoelectric properties, and surface morphology with different solvent ratios of DMSO and acetone.

EXPERIMENTAL

Materials and Methods

The precursor solution (4.0 vol %) was prepared by dissolving 75 g of PVDF (Sigma-Aldrich, Co., 182702-100G) in various mixed solvents (10 mL) with ratios of acetone to dimethyl sulfoxide (DMSO) of 5 : 5, 6 : 4, 7 : 3, 8 : 2, 9 : 1, and 10 : 0. PVDF solutions were cast into porous alumina membrane templates (Whatman) with average pore sizes of 200 nm. For the infiltration of the PVDF solution into the AAO pores, the AAO template was placed in a vacuum chamber for 10 min at room temperature and then dried at 60°C under ambient conditions for 10 h. Subsequently, the AAO templates were dissolved in aqueous 5*M* NaOH. After removing the templates, the samples were rinsed with water and dried at 50°C. Finally, vertically aligned PVDF mesoscale rod arrays were obtained. For piezoresponse force microscopy (PFM) measurements, the PVDF rod arrays were dispersed in water and each rod was placed on a Pt/Si substrate.

Measurements

PFM domain imaging was performed using commercially available Pt-coated Si tips with a tip apex radius of 40 nm (Mikromasch, spring constant $k \sim 6.0$ N/m).[33,34] The piezoresponse hysteresis loops were obtained using a commercial AFM (XE-100, Park Systems, Korea) equipped with a lock-in amplifier (SR 830, Stanford Research System) and the Labview program. The local hysteresis loops, measured at ten random positions on top of each rod, were averaged. SEM images were obtained using a HITACHI S-4800 (Field emission type) scanning electron microscope at 10 kV. For verification of the crystal phases of the rod structures, grazing angle X-ray diffraction (GAXRD) measurements, and grazing incidence reflection absorption Fourier transform infrared spectroscopy (GIRA-FTIR) were performed. XRD measurements were done using a RIGAKU D/MAX-2500 at a scanning velocity of 1°/min (40 kV, 300 mA); for detecting only the rods we used a 2θ scan in which the collimated incidence beam was fixed at a grazing angle of 2° while the detector scanned over the selected angle range. FTIR spectra were obtained using a Bruker Optiks IFS66V/S and a HYPERION 3000.

In order to determine the interfacial energies between the wetting solutions and the surface of the AAO template, an Al_2O_3 plate (99.8%) was used instead of the AAO templates. The contact angles between the mixed solutions and the Al_2O_3 plate were obtained using a pendant drop tensiometer (KRUSS GmbH, DSA 100). The surface tension and viscosity of the mixed solutions were obtained using a du Nüoy ring tensiometer (KRUSS, K1001) and a viscometer (RheoSense, Lab-VROC), respectively.

RESULTS AND DISCUSSION

Surface Morphology of PVDF Mesoscale Structures

Vertically aligned PVDF mesoscale structures were fabricated using the porous template technique with various solvents; the ratios of acetone to DMSO were 5 : 5, 6 : 4, 7 : 3, 8 : 2, 9 : 1, and 10 :0 [Figure 1 (top view only, cross-section images are included in Supporting information)]. The PVDF rods became shorter and thicker as the acetone concentration decreased. The average heights of the rods with solvent ratios of 5 : 5, 7 : 3, and 10 : 0 were 3.82, 1.68, and 1.09 μm, respectively (the standard deviations were 1.18, 0.24, and 0.19 μm, respectively). These results can be interpreted using the Lucas–Washburn equation.[35] The distance of penetration x at time t can be expressed as:

$$x = \sqrt{\frac{\gamma_{LV} R \cos\theta_t}{2\eta}} \quad (1)$$

where γ_{LV} is the surface tension of the liquid having viscosity η, θ is the contact angle between the liquid and the capillary wall, and R is the radius of the rod. The infiltration depth, x, is proportional to the square root of the product of γ_{LV} and cos θ, and inversely proportional to the square root of η. The values of γ_{LV}, θ, and η of the solutions used in this study are listed in Table I. Importantly, as the ratio of acetone in the solution decreased, both γ_{LV} and cos θ showed similar trends, but the viscosity of the solutions increased sharply. In our case, we believe the viscosity is the most important factor because not only did the viscosity show the largest variation among the experimental parameters, but also the viscous force is dominant for pores with very small radii.[33] Consequently, a solution of low viscosity produces longer rods than does a highly viscous

Applied Polymer SCIENCE

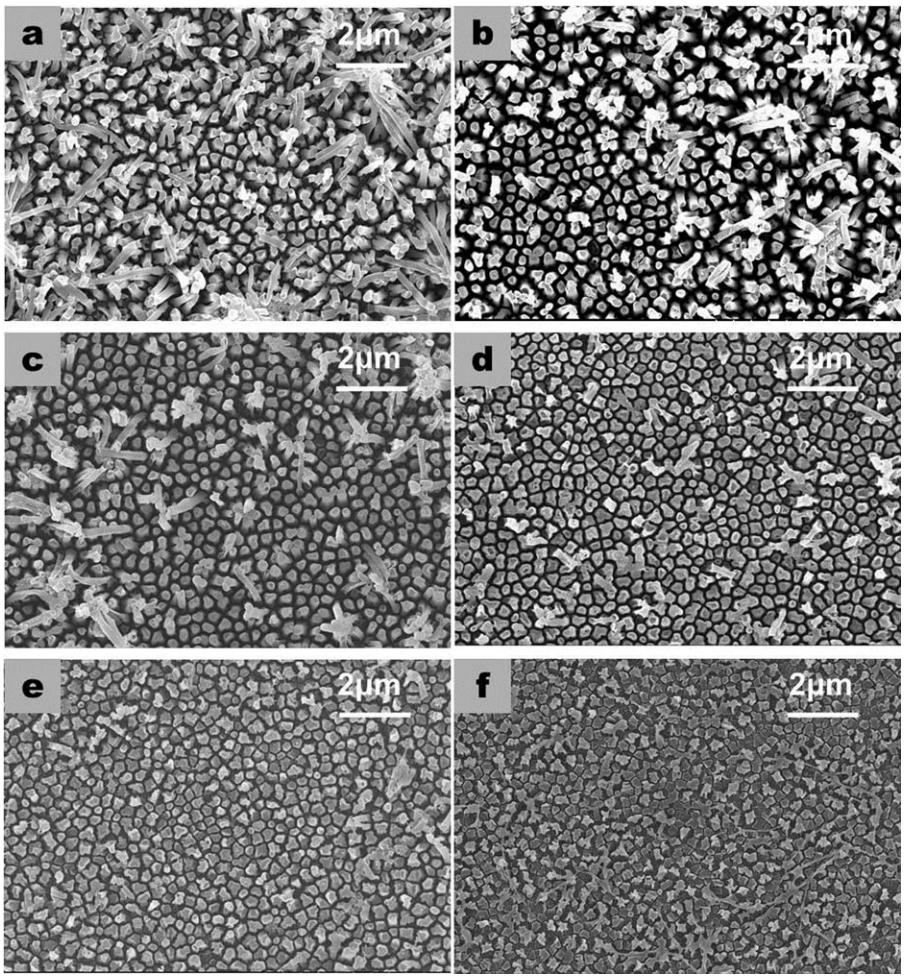

Figure 1. Top-view SEM images of PVDF mesoscale structures using solvents with DMSO : acetone ratios of (a) 5 : 5, (b) 6 : 4, (c) 7 : 3, (d) 8 : 2, (e) 9 : 1, and (f) 10 : 0.

solution because the former infiltrates more than the latter does.

The average diameter of the rods with solvent ratios of 5 : 5, 6 : 4, 7 : 3, 8 : 2, 9 : 1, and 10 : 0 were 232, 234, 258, 283, 288, and 287 nm, respectively (the standard deviations were 0.014, 0.042, 0.028, 0.038, 0.037, and 0.075 nm, respectively). We conducted an analysis of variance (ANOVA) test to verify if the increase in diameter as a function of solvent ratio is statistically meaningful (Supporting Information); it was found that the diameter increases with the solvent ratio at a 0.1 level of statistical significance. The reasons why the diameter of the PVDF rods exceeds that of AAO and increases as a function of the solvent ratio are not clearly understood at this stage. One possible scenario is that as the viscosity of the solvent increases when the ratio between DMSO and acetone changes from 5 : 5 to 10 : 0, the porosity in the crystallized rods decreases,[36] which enhances the apparent density, thereby leading to an increase in residual stress inside the AAO pores. Therefore, once we remove AAO, the rods will expand in proportion to the residual stress, which is in agreement with the diameter change as a function of the ratio between DMSO and acetone, as shown in Figure 2.

Table I. Values of Measurement of Rheology Properties of the Solutions

				H (cP)			
DMSO : acetone	γLV (mN/m)	θ (°)	cos θ	250/s (shear rate)	400/s	550/s	700/s
50 : 50	32.8	30.34	0.86	102	105	102	99.5
70 : 30	35.3	21.32	0.93	137	136	132	129
100 : 0	41.0	15.88	0.96	233	217	206	192

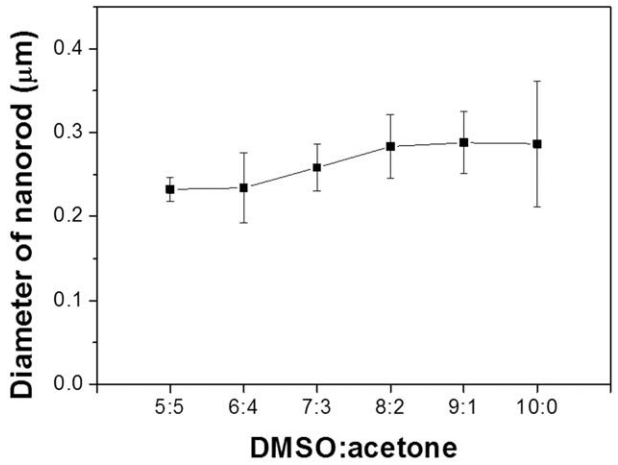

Figure 2. Plot of average diameter of PVDF rods with different solvent ratios in terms of DMSO : acetone. Error bars represent the standard deviations.

Crystalline Phase Characterization of PVDF Mesoscale Rods Arrays

In order to verify that the processing recipe for enhancing the β phase in the bulk structures is equally applicable to the synthesis of rods, we conducted FTIR and XRD experiments on the rods fabricated from solutions comprised of DMSO and acetone with different volume ratio. FTIR spectra [Figure 3(a)] for various ratios of DMSO and acetone show that all the rods were associated mainly with ferroelectric β and γ phases,[4,30,37–40] which is also the case with bulk samples (Supporting Information). We believe there is an insignificant amount of α phase in the rods, as manifested by the relatively small peak at the wavenumber of 615 cm^{-1} and the absence of peaks at the wavenumbers of 764, 795, 855, 976, 1210, 1383, and 1423 cm^{-1}, which are the characteristic bands of the α phase.

Based on our findings that all the rods consist mainly of β and γ phases, we calculated the peak intensity ratio between the band at 1273 cm^{-1} (β phase) and that at 1233 cm^{-1} (γ phase) in order to measure the relative volume ratio of the β and γ phases. The peak ratio is about 0.65 when the ratio between DMSO and acetone is 5 : 5; this peak ratio stays nearly constant until the ratio between DMSO and acetone reaches 9 : 1. When we use only pure DMSO, the peak ratio jumps to about 1.1 [Figure 3(b)]. This indicates that the rods formed using 100% pure DMSO contains more β phase than those formed using mixed solvents. When compared with bulk samples fabricated from the same ratio of DMSO and acetone, we find that the overall qualitative trend is similar to that of rods in which the peak ratio is around 0.6 for the DMSO/acetone ratio ranging from 5 : 5 to 9 : 1; that peak ratio increases to 0.8 when the DMSO/acetone ratio is 10 : 0.

It is well-known that the amount of β phase increases in PVDF films as the dipole moment of the solvents increases and the rate of evaporation decreases. Therefore, we may understand why we observe more β phase in solution with the ratio of 10 : 0 than we do in a solution with a 9 : 1 ratio between DMSO and acetone. In Table II, acetone has lower polarity (i.e., the dipole moments of DMSO and acetone are 3.96 and 2.88 D,

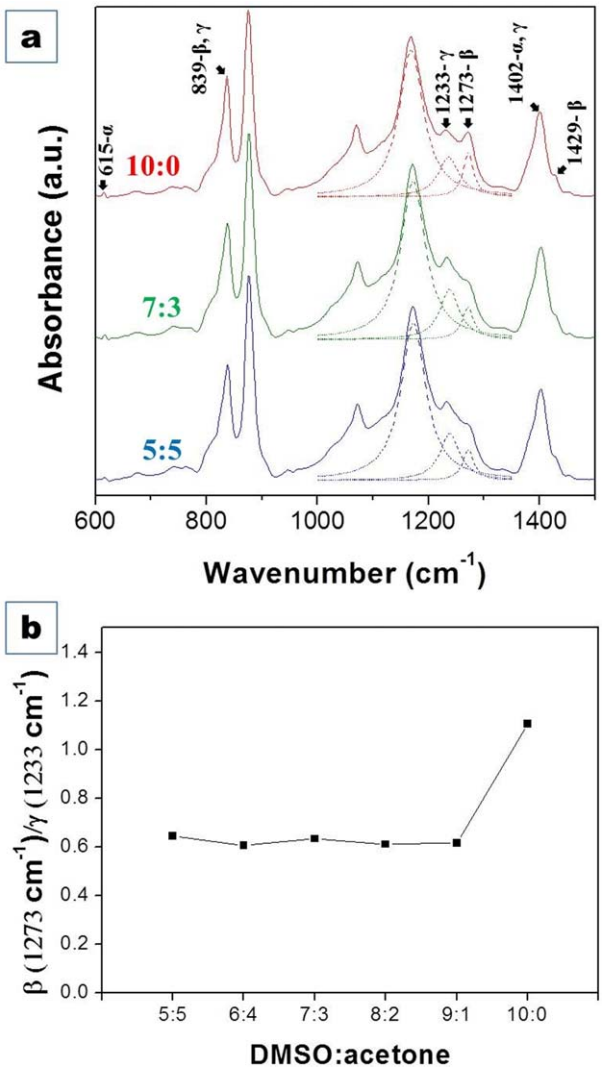

Figure 3. (a) FTIR spectra of PVDF rods formed using mixed solvents in which ratios of DMSO to acetone are 10 : 0, 7 : 3, and 5 : 5. (b) Plot of the ratio between the bands at 1273 cm^{-1} (β phase) and at 1233 cm^{-1} (γ phase). [Color figure can be viewed in the online issue, which is available at wileyonlinelibrary.com.]

respectively), and has higher vapor pressure than DMSO (i.e., the vapor pressures of DMSO and acetone are 0.056 and 185 kPa, respectively). However, it is not clear why the relative amount of β phase remains constant for the ratio range from 5 : 5 to 9 : 1, regardless of the amount of acetone added to the solution.

In order to complement the FTIR results, in which we found mainly β and γ phases in the rods, we conducted XRD experiments to verify the crystallinity of the phases (Figure 4). In the XRD patterns, the prominent peaks near $2\theta = 20°$ are located at $2\theta = 20.26°$, $2\theta = 20.18°$, and $2\theta = 20.14°$ for crystallized PVDF rods made from mixtures with DMSO contents of 100, 70, and 50 vol %, respectively. This peak is the sum of the (110/200) β and the (110) γ reflections.[30,32,38,41] The small peak at $2\theta = 36.25°$ (all the same peak) is the sum of the (020/101) β and the (200) γ reflections.[39,42] Therefore, based on both

Table II. Properties of DMSO and Acetone[a]

At 20°C	Density (g/cm^3)	Viscosity (cP)	Surface tension (mN/m)	Melting/boiling temperature (°C)	Vapor pressure (kPa)	Dipole moment (D)
DMSO	1.1004	1.996	43.54	18.5/189	0.056	3.96
Acetone	0.7925	0.3075	23.29	−94.9/56.53	185	2.91

[a] CRC Handbook of Chemistry and Physics, CRC Press, 2000.

FTIR and XRD results, we were able to confirm that the PVDF rods contain mostly β and γ crystalline phases.

Piezoelectric Properties of PVDF Mesoscale Rods

Based on the structure analysis performed using FTIR and XRD, we expect that the rods fabricated using our recipe will exhibit ferroelectric/piezoelectric properties close to those of bulk PVDF due to the high relative amount of β phase. One unknown factor is the amount of amorphous phase, which would deteriorate the overall ferroelectric/piezoelectric properties. In order to validate our argument that we can apply the recipe developed for bulk samples to the synthesis of mesoscale ferroelectric rods, we measured the local piezoresponse hysteresis loops of the PVDF rods.

Figure 5(a) and (b) shows a schematic of the PFM imaging and the PFM domain images of a rod fabricated using 100% DMSO. It should be noted that we were not able to image all the rods due to the challenges involved with soft materials and the complex geometry of rods; however, we ensured that the PFM tip remained in contact with each rod when we measured the local piezoresponse hysteresis loops (Figure 6).

Remnant piezoresponse ($d_{33,r}$) values for PVDF rods from the mixtures of DMSO and acetone with ratios of 5 : 5, 7 : 3, and 10 : 0 were −2.12 , −3.06, and −5.04 pm/V, respectively [β phase PVDF has piezoelectric coefficients of approximately

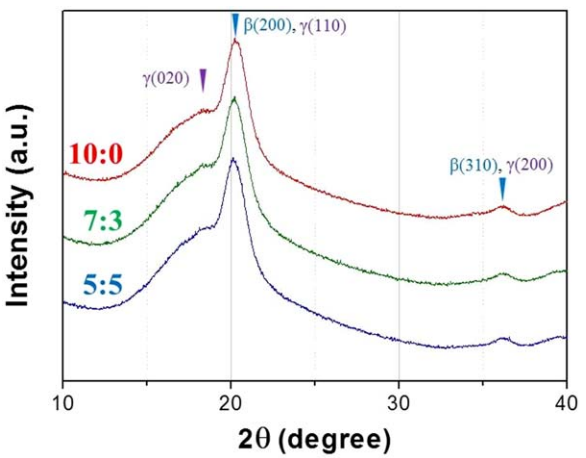

Figure 4. XRD pattern of PVDF rods formed using mixed solvents in which ratio of DMSO to acetone are 10 : 0, 7 : 3, and 5 : 5. [Color figure can be viewed in the online issue, which is available at wileyonlinelibrary.com.]

−20 to 35 (d_{33})],[43,44] the coercive voltage values were 2.32, 2.29, and 2.71 V, respectively. It is quite clear that the absolute value of the remnant piezoresponse increased when we used pure DMSO; we may understand the reason behind this increase as being due to the fact that the relative amount of β phase is higher when we use pure DMSO as the solvent than when we use a mixture of DMSO and acetone, as shown in Figure 3(b). However, this argument does not seem to work when we compare the cases in which we added different amounts of acetone to the solution, because the absolute value of the remnant piezoresponse increased from 2.12 to 3.06 pm/V even though the relative amount of β phase remained constant.

We speculate that the absolute amount of crystalline β phase should be measured to obtain an overall picture of what is responsible for the increase as a function of the ratio between DMSO and acetone. If we assume that our rods consist of ferroelectric crystalline β and γ phases and non-ferroelectric amorphous phase (a so called dead layer), then we may interpret our results in terms of increase in overall crystalline ferroelectric β phase inside the rods when we add more DMSO to the solution. This is supported by the fact that both the slope of the d_{33} versus V plot and the remnant piezoresponse increase as we increase the relative amount of DMSO in the solution.[45] The slope of the hysteresis loops in the coercive field decreases as the dead layer thickness increases, which acts like a low permittivity capacitor connected in series with the polymer ferroelectrics. This layer also decreases the overall electric field that induces piezoelectric strain in the ferroelectric polymer, which decreases the remnant piezoresponse. More direct evidence will be provided by on-going research on quantitative evaluation of the amorphous phase in PVDF structures using XRD, FTIR, and TEM; this research is currently underway in our group.

CONCLUSIONS

We have fabricated vertically aligned ferroelectric PVDF mesoscale rod arrays comprised of β and γ phases using the porous template technique. We were able to synthesize a ferroelectric phase in the form of a rod by combining the well-established recipe for crystallizing the β phase using DMSO at low temperature and template-guided infiltration processing for rods using AAO. We were able to control the length of rods in a range from 3.82 to 1.09 μm and the diameters from 232 to 287 nm by changing the volume ratio between DMSO and acetone from 5 : 5 to 10 : 0. We obtained well-defined piezoresponse hysteresis loops for all rods with remnant piezoresponse ranging from −2.12 to −5.04 pm/V and coercive voltage ranging from

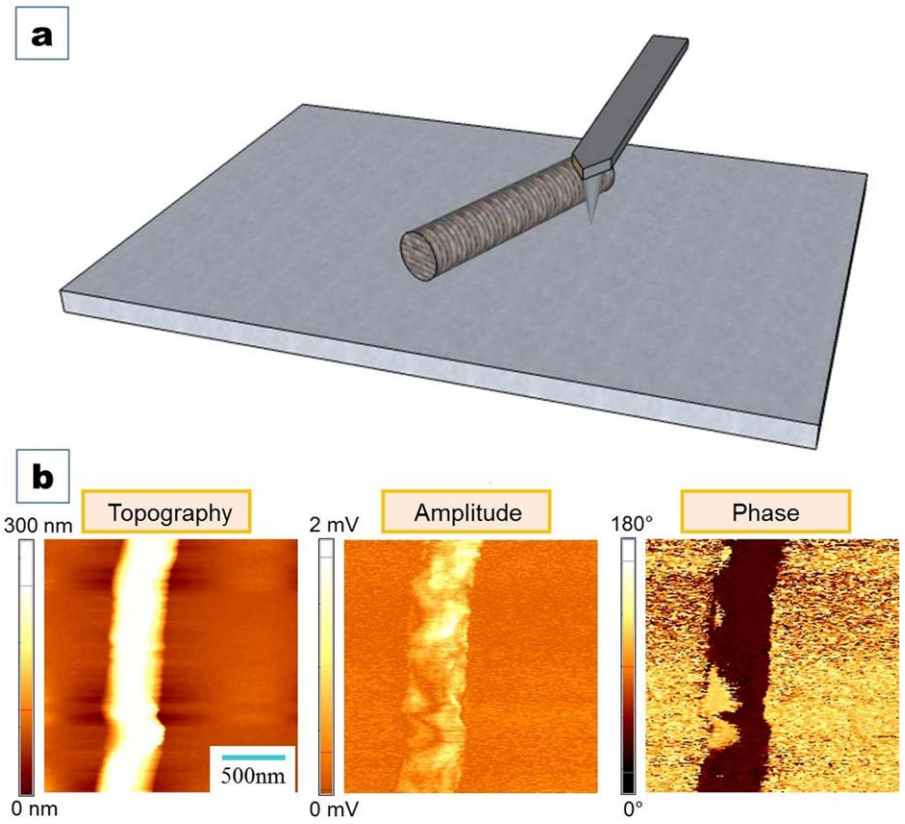

Figure 5. (a) Schematic of PFM experiments on PVDF rods. (b) Topography, PFM amplitude, and phase images of PVDF rod made from solvent with 100% DMSO. [Color figure can be viewed in the online issue, which is available at wileyonlinelibrary.com.]

2.29 to 2.71 V. Our results serve as a processing platform for flexible electronic devices that need high capacitance with piezoelectric functionality, such as body energy harvesting devices for intelligent systems.

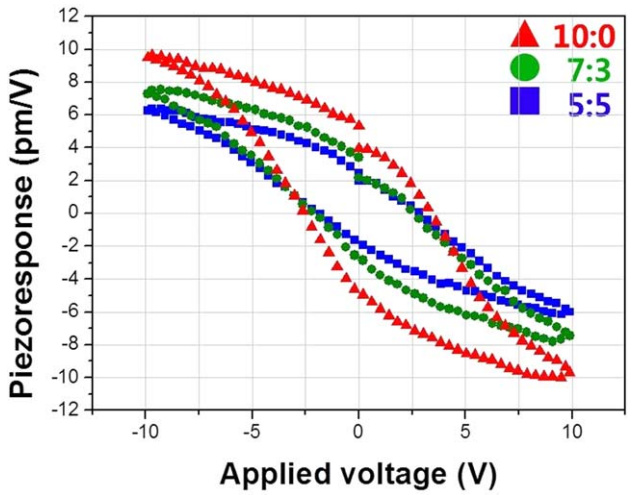

Figure 6. Local piezoresponse hysteresis loops; triangle: DMSO 100%; circle: DMSO 70% and acetone 30%; square: DMSO 50% and acetone 50%. [Color figure can be viewed in the online issue, which is available at wileyonlinelibrary.com.]

ACKNOWLEDGMENTS

This research was supported by the Mid-career Researcher Program (No. 2010-0015063) and the Conversion Research Center Program (No. 2011K000674) through the National Research Foundation of Korea (NRF) funded by the Ministry of Education, Science and Technology (MEST) and by a New and Renewable Energy of the Korea Institute of Energy Technology Evaluation and Planning (KETEP) grant (No. 20103020060010) funded by the Ministry of Knowledge Economy, Korea. Work at Argonne National Laboratory (S.H., D.K. and Y.C., data analysis and writing of manuscript) was supported by UChicago Argonne, a US DOE Office of Science Laboratory, operated under Contract No. DE-AC02-06CH11357. J.H. acknowledges Chung-Ang University Research Grants in 2011.

REFERENCES

1. Gelinck, G. H.; Marsman, A. W.; Touwslager, F. J.; Setayesh, S.; de Leeuw, D. M.; *Appl. Phys. Lett.* **2005**, *87*, 092903.
2. Ducharme, S. *IEEE Trans. Device Mater. Reliab.* **2005**, *5*, 720.
3. Sharma, P.; Reece, T. J.; Ducharme, S.; Gruverman, A. *Nano Lett.* **2011**, *11*, 1970.
4. Unni, K. N. N.; Bettignies, R.; Dabos-Seignon, S.; Nunzi. J. *Appl. Phys. Lett.* **2004**, *85*, 1823.

5. Taylor, G. W.; Burns, J. R.; Kammann, S. M.; Powers, W. B.; Welsh, T. R. *IEEE J. Oceanic Eng.* **2001**, *26*, 539.
6. Kressmann, R. *J. Acoust. Soc. Am.* **2001**, *109*, 1412.
7. Bauer, S.; Gerhard-Multhaupt, R.; Sessler, G. M. *Phys. Today* **2004**, *57*, 37.
8. Tzou, H. S.; Tseng, C. I. *J. Sound Vib.* **1990**, *138*, 17.
9. Lee, C. K. *J. Acoust. Soc. Am.* **1990**, *87*, 1144.
10. Hu, Z.; Tian, M.; Nysten, B.; Jonas, A. M. *Nat. Mater.* **2009**, *8*, 62.
11. Wang, X.; Song, J.; Liu, J.; Wang, Z. L. *Science* **2007**, *316*, 102.
12. Xia, Y.; Yang, P.; Sun, Y.; Wu, Y.; Mayers, B.; Gates, B.; Yin, Y.; Kim, F.; Yan, H. *Adv. Mater.* **2003**, *15*, 353.
13. Steinhart, M.; Göring, P.; Dernaika, H.; Prabhukaran, M.; Gösele, U. *Phys. Rev. Lett.* **2006**, *97*, 027801.
14. Steinhart, M.; Wehrspohn, R. B.; Gösele, U.; Wendorff, J. H. *Angew. Chem. Int. Ed.* **2004**, *43*, 1334.
15. Martin, C. R. *Science* **1994**, *266*, 1961.
16. Kang, S.; Park, Y.; Bae, I.; Kim, K.; Kim, H.; Bauer, S.; Thomas, E. L.; Park, C. *Adv. Funct. Mater.* **2009**, *19*, 2812.
17. Loo, Y.; Register, R. A. *Phys. Rev. Lett.* **2000**, *84*, 4120.
18. Martín, J.; Mijangos, C. *Langmuir* **2009**, *25*, 1181.
19. García-Gutiérrez, M.; Linares, A.; Hernández, J. J.; Rueda, D. R.; Ezquerra, T. A.; Poza, P.; Davies, R. J. *Nano Lett.* **2010**, *10*, 1472.
20. Lin, J.; Lu, S. G.; Lin, M.; Geu, M.; Zhang, Q. M. *Appl. Phys. Lett.* **2009**, *95*, 022911.
21. Lovinger, A. J. *Science* **1983**, *220*, 1115.
22. Bliznyuk, V. N.; Baig, A.; Singamaneni, S.; Pud, A. A.; Fatyeyeva, K. Y.; Shapoval, G. S. *Polymer* **2005**, *46*,11728.
23. Ray, S.; Easteal, A. J.; Cooney, R. P.; Edmonds, N. R. *Mater. Chem. Phys.* **2009**, *113*, 829.
24. Tashiro, K.; Tadokoro, H.; Kobayashi, M. *Ferroelectrics* **1981**, *32*, 167.
25. He, X.; Yao, K. *Appl. Phys. Lett.* **2006**, *89*, 112909.
26. Tashiro, K.; Itoh, Y.; Kobayashi, M.; Tadokoro, H. *Macromolecules* **1985**, *18*, 2600.
27. Kaurat, T.; Natht, R.; Perlman, M. M. *J. Phys. Part D: Appl. Phys.* **1991**, *24*, 1848.
28. Hsu, S. L.; Lu, F. J.; Waldman, D. A.; Muthukumar, M. *Macromolecules* **1985**, *18*, 2583.
29. Gregorio Jr., R. *J. Mater. Sci.* **1999**, *34*, 4489.
30. Gregorio Jr., R.; Borges, D. S. *Polymer* **2008**, *49*, 4009.
31. Zhao, X.; Cheng, J.; Chen, S.; Zhang, J.; Wang, X. *J. Polym. Sci. Part B: Polym. Phys.* **2010**, *10*, 1002.
32. Ma, W.; Zhang, J.; Chen, S.; Wang, X. *J. Polym. Sci. Part B: Polym. Phys.* **2008**, *47*, 434.
33. Hong, S.; Woo, J.; Shin, H.; Jeon, J. U.; Pak, Y. E.; Colla, E. L.; Setter, N.; Kim, E.; No, K. *J. Appl. Phys.* **2001**, *89*, 1377.
34. Hong, S.; Shin, H.; Woo, J.; No, K. *Appl. Phys. Lett.* **2002**, *80*, 1453.
35. Martic, G.; Gentner, F.; Seveno, D.; Coulon, D.; De Coninck, J. *Langmuir* **2002**, *18*, 7971.
36. Li, Q.; Xu, Z.; Yu, L. *J. Appl. Polym. Sci.* **2010**, *115*, 2277.
37. Kim, K. J.; Reynolds, N. M.; Hsu, S. L. *Macromolecules* **1989**, *22*, 4395.
38. Gregorio Jr., R. *J. Appl. Polym. Sci.* **2006**, *100*, 3272.
39. Benz, M.; Euler, W. B. *J. Appl. Polym. Sci.* **2003**, *89*, 1093.
40. Benz, M.; Euler, W. B.; Gregory, O. J. *Macromolecules* **2002**, *35*, 2682.
41. Takahashi, N.; Odajima, A. *Ferroelectrics* **1981**, *32*, 49.
42. Mohammadi, B.; Yousefi, A. A.; Bellah, S.M. *Polym. Test.* **2007**, *26*, 42.
43. Rietveld, I. B.; Kobayashi, K.; Honjo, T.; Ishida, K.; Yamada, H.; Matsushige, K. *J. Mater. Chem.* **2010**, *20*, 8272.
44. Sun, C.; Shi, J.; Bayer, D. J.; Wang X. *Energy Environ. Sci.* **2011**, *4*, 4508.
45. Yoo, I. K. In Nanoscale Phenomena in Ferroelectric Thin Films; Hong, S. Eds.; Kluwer Academic Publishers: Boston, **2004**; Chapter 1.4.